

Article

Self-Assembled Amphiphilic Chitosan Nanomicelles: Synthesis, Characterization and Antibacterial Activity

Yi Qi ^{1,2,3,†}, Qizhou Chen ^{1,†}, Xiaofen Cai ¹, Lifen Liu ¹, Yuwei Jiang ¹, Xufeng Zhu ^{1,2}, Zhicheng Huang ¹, Kefeng Wu ^{1,2,3,*}, Hui Luo ^{1,2,3} and Qianqian Ouyang ^{1,2,3,*} 

¹ Marine Biomedical Research Institution, Guangdong Medical University, Zhanjiang 524023, China; qiyi7272@gdmu.edu.cn (Y.Q.); sj13423409060@gmail.com (Q.C.); 13413676045@163.com (X.C.); 15125044514@163.com (L.L.); jyw20000215@163.com (Y.J.); xufeng910730@126.com (X.Z.); 498556764@163.com (Z.H.); luohui@gdmu.edu.cn (H.L.)

² The Marine Biomedical Research Institute of Guangdong Zhanjiang, Zhanjiang 524023, China

³ The Key Lab of Zhanjiang for R&D Marine Microbial Resources in the Beibu Gulf Rim, Marine Biomedical Research Institute, Guangdong Medical University, Zhanjiang 524023, China

* Correspondence: winvee@gdmu.edu.cn (K.W.); oyqq617@gdmu.edu.cn (Q.O.)

† These authors contributed equally to this work.

Abstract: Although amphiphilic chitosan has been widely studied as a drug carrier for drug delivery, fewer studies have been conducted on the antimicrobial activity of amphiphilic chitosan. In this study, we successfully synthesized deoxycholic acid-modified chitosan (CS-DA) by grafting deoxycholic acid (DA) onto chitosan C₂-NH₂, followed by grafting succinic anhydride, to prepare a novel amphiphilic chitosan (CS-DA-SA). The substitution degree was 23.93% for deoxycholic acid and 29.25% for succinic anhydride. Both CS-DA and CS-DA-SA showed good blood compatibility. Notably, the synthesized CS-DA-SA can self-assemble to form nanomicelles at low concentrations in an aqueous environment. The results of CS, CS-DA, and CS-DA-SA against *Escherichia coli* and *Staphylococcus aureus* showed that CS-DA and CS-DA-SA exhibited stronger antimicrobial effects than CS. CS-DA-SA may exert its antimicrobial effect by disrupting cell membranes or forming a membrane on the cell surface. Overall, the novel CS-DA-SA biomaterials have a promising future in antibacterial therapy.

Keywords: deoxycholic acid; succinic anhydride; amphiphilic chitosan; nanomicelles; antibacterial activity



Citation: Qi, Y.; Chen, Q.; Cai, X.; Liu, L.; Jiang, Y.; Zhu, X.; Huang, Z.; Wu, K.; Luo, H.; Ouyang, Q.

Self-Assembled Amphiphilic Chitosan Nanomicelles: Synthesis, Characterization and Antibacterial Activity. *Biomolecules* **2023**, *13*, 1595. <https://doi.org/10.3390/biom13111595>

Academic Editor: Annarita Falanga

Received: 21 September 2023

Revised: 19 October 2023

Accepted: 28 October 2023

Published: 30 October 2023



Copyright: © 2023 by the authors. Licensee MDPI, Basel, Switzerland. This article is an open access article distributed under the terms and conditions of the Creative Commons Attribution (CC BY) license (<https://creativecommons.org/licenses/by/4.0/>).

1. Introduction

In recent years, due to the misuse of antibiotics by humans, many microorganisms have become highly resistant to commonly used antibiotics, which has led to increased morbidity and mortality from infectious diseases and has also become a serious public health problem worldwide [1,2]. Due to the long time, high cost, and little effect required to discover new antimicrobial agents from natural products, increasing attention is being paid to the use of synthetic compounds with antimicrobial activity. Natural antimicrobial polymers are biocompatible, biodegradable, safe, and non-toxic, and can exert antibacterial or bactericidal effects through their chemical structures, making them a new generation of antimicrobial agents [3]. Currently, nanomaterials have developed as promising materials in various fields of science and technology. In particular, they have become the most widely used materials in medical practice [4]. Nanomaterials have been widely used in wastewater treatment, antimicrobials, photothermal therapy, biomedical imaging, and cancer treatment [5,6]. To address the problem of antibiotic resistance, more and more researchers are working on developing alternatives to traditional antibiotics. Compared with antibiotics, nanomaterials can produce synergistic antimicrobial effects through multiple mechanisms of action and can act on specific targets within the bacterial cell, reducing the risk of resistance development [7]. Nanomaterials have the advantages of broad-spectrum

antibacterials, high efficiency, and low toxicity, and can play an antibacterial role by destroying bacterial cell membranes or interfering with bacterial physiological activity [8]. For example, A.F. Jafarova et al. [9] prepared environmentally friendly and non-toxic silver nanoparticles using biological methods and investigated their antibacterial activity against *Bacillus subtilis* and *Staphylococcus aureus*, and the results showed that silver nanoparticles with sizes in the range of 50–100 nm can solubilize the bacteria and produce a good antibacterial effect.

Chitosan is the only known and abundant natural basic cationic polymer [10]. It has positively charged amino groups that bind to their anionic counterparts in the mucous membrane layer and can be administered through the gastrointestinal tract, skin, and nasal passages [11]. Chitosan has good biodegradability, biocompatibility, and cellular affinity [12,13]. Chitosan has rich pharmacological effects such as antibacterial, hemostatic, antiviral, and inhibitory effects on a wide range of bacteria and fungi [14–16]. Studies have shown that the antibacterial principle of chitosan may result from electrostatic interactions between its positively charged amino group and negative charges present on microbial membranes, resulting in antibacterial effects [17]. However, chitosan is poorly water-soluble and has a weak positive charge; thus, the antimicrobial activity is weak [18,19]. The antimicrobial properties of chitosan are associated with various factors, including molecular weight, pH, temperature, and the extent of deacetylation [20], and its antimicrobial activity is unstable, so its application in the antimicrobial field is limited. The chemical properties of $-NH_2$ and $-OH$ of chitosan molecular chains are active and can be chemically modified to synthesize chitosan derivatives [21]. More and more studies have shown that chitosan derivatives synthesized by the chemical modification of chitosan can enhance its antimicrobial activity [22,23]. For example, Fengling Tang et al. [24] used succinic anhydride and basic chitosan as raw materials for the synthesis of N-succinyl chitosan (NSC), a water-soluble derivative of chitosan, finding that CS solubility was markedly enhanced by NSC, together with excellent antibacterial properties and antimicrobial activity. NSC reduced bacterial infection and promoted the formation of granulation tissue and epithelialization in rabbit skin wounds, with markedly shorter healing times relative to CS. Nurazimah Ahmad et al. [25] synthesized amphiphilic chitosan (CH-Arg-OA) by grafting arginine and oleic acid through a carbodiimide-mediated reaction and investigated its antimicrobial activity, and the resultant CH-Arg-OA showed significant antibacterial action, particularly against gram-negative bacteria. These effects were due to disruption of the outer membranes of the bacteria, minimizing the possibility of bacterial drug resistance.

The structure of amphiphilic chitosan has both hydrophilic and hydrophobic groups, which can self-assemble to form super-stable nanomicelles when dissolved in water [26,27], leading to increased stability of the antimicrobial action of the amphiphilic chitosan nanomicelles. The present study aimed to improve both the antibacterial properties and stability of chitosan and thus synthesized amphiphilic chitosan using the hydrophobic modification of chitosan with deoxycholic acid and the hydrophilic modification of chitosan with succinic anhydride. Deoxycholic acid is often used as a hydrophobic group for the hydrophobic modification of amphiphilic polymers, and has strong antimicrobial activity [28]. Succinic anhydride can be hydrolyzed to succinic acid, which is strongly acidic, allowing high nanocellulose yields to be achieved [29]. Succinic anhydride is commonly used for the hydrophilic modification of chitosan, and its synthetic product, N-succinyl chitosan, also has good antibacterial activity [24]. The CS-DA-SA structure was characterized by nuclear magnetic resonance hydrogen spectroscopy, Fourier-transform infrared spectroscopy, and X-ray diffraction. Ultrasonication reduces aggregation and releases individual particles, reducing viscosity between materials [30]. Ultrasonic self-assembly was used to prepare the amphiphilic chitosan nanomicelles (CS-DA-SA-NMs), and their sizes, zeta potentials, and microscopic structures were investigated. The antibacterial properties of CS, CS-DA, and CS-DA-SA were compared and analyzed, and the possible mechanisms of their antibacterial effects were discussed. In this paper, novel amphiphilic polymeric nanomicelles were prepared to improve the antibacterial activity and stability of chitosan.

2. Experimental

2.1. Materials

Chitosan (CS, viscosity < 200 mPa.s, 97.8% deacetylated), N-acetyl-L-cysteine (NAC), 1-ethyl-3(3-dimethylaminopropyl) carbodiimide hydrochloride (EDAC), deoxycholic acid (DA), and succinic anhydride (SA) were purchased from Macklin (Shanghai, China). Both *E. coli* (CMCC(B) 44103) and *S. aureus* (ATCC 25923) were from the China Center of Industrial Culture Collection, Beijing, China. In addition, methanol, ammonia, glacial acetic acid, ethanol, acetone, and DMSO were from Guanghai Technology Co., Ltd. (Shantou, China). The reagents and chemicals were all of analytical grade and were not further purified. All experiments used ultrapure water.

2.2. Synthesis of Chitosan Derivatives

2.2.1. CS-DA Synthesis

Referring to the modified method in the literature [31], a clean 250 mL beaker was taken, to which 75 mL of 1% acetic acid solution and 0.5 g chitosan were added sequentially and stirred to dissolve chitosan completely. Take another beaker and add 75 mL of methanol and 1.217 g of deoxycholic acid, then add 0.296 g of EDAC and 0.538 g of NHS, respectively, and stir for 2 h for activation. After activation, transfer it into a chitosan solution. If milky turbidity appears, add some methanol to dissolve it, and stir the reaction for 24 h at ambient temperature. Then, add ammonia while stirring until the product is completely at the end of the reaction. Let it stand for 5 min and then filter. Wash with anhydrous ethanol and filter and repeat 3 times. Dry under a vacuum to obtain deoxycholic acid-modified chitosan (CS-DA). Details of the synthesis are shown in Figure S1.

2.2.2. CS-DA-SA Synthesis

Referring to the modified method in the literature [32], 0.25 g CS-DA was weighed, followed by dissolution in 50 mL of 1% acetic acid, and another 0.166 g succinic anhydride was weighed and dissolved in 20 mL of acetone, followed by a dropwise addition of the succinic anhydride/acetone solution to CS-DA with constant stirring for 4 h at 40 °C. After the reaction, excess acetone was added until the product was complete. After the reaction, add excess acetone until the product is completely analyzed, and then filter and wash the solid phase with 70%, 80%, and 100% acetone, respectively, and dry it under a vacuum for 24 h. The amphiphilic chitosan (CS-DA-SA) is obtained. Details of the synthesis are shown in Figure S2.

2.3. Identification and Characterization of Compounds

FTIR spectra of the chitosan and derivatives were obtained using the potassium bromide compression method. ¹H NMR spectra at 400 MHz were obtained using a Bruker AVANCE NEO 400 MHz spectrometer. CS, CS-DA, and CS-DA-SA were dissolved in a mixture of D₂O and C₂D₄O₂. The crystallization behavior of chitosan and its derivatives were analyzed by a Rigaku Smart Lab 9 kW X-ray diffractometer with scanning angles of 10°–80°.

2.4. Determination of the Grafting Rate

2.4.1. DA Grafting Rate

The rate of deoxycholic acid grafting on chitosan can be quantified by reacting the chitosan-free amino group with ninhydrin [33]. Five chitosan solutions were prepared at concentrations of 0.25, 0.5, 1, 2, and 4 mg/mL, respectively. Assuming that the concentration of 4 mg/mL chitosan has 100% free amino acid, the other four chitosan solutions have 50%, 25%, 12.5%, and 6.25% free amino acid (C), respectively. Take 0.5 mL of each of the above chitosan solutions, add 0.5 mL of an acetate buffer (pH 5.5) and 2 mL of aqueous ninhydrin (5 mg of ninhydrin, dissolved in 100 mL of ethanol) dropwise, heat mixed solutions in a water bath at 90 °C, and stir magnetically for 15 min. Absorbances (A) at 570 nm were determined on a UV spectrophotometer. Linear regression of A and C was determined as

$C = aA + b$. The absorbance of a 2 mg/mL solution of a CS-DA solution was measured. From the linear regression equation $C = aA + b$, the corresponding amount of free amino acid could be calculated, and the grafting rate of CS-DA is $100\% - C$.

2.4.2. SA Grafting Rate

The C, H, and N contents in CS-DA and CS-DA-SA were determined by the Dumas combustion method using an Elementar vario EL cube organic elemental analyzer. The amount of SA substitution was evaluated using Equation (1).

$$DS = \frac{C/N_{CS-DA-SA} - C/N_{CS-DA}}{C/N_{SA-DA-GCA} - C/N_{GCA}} \quad (1)$$

where $C/N_{SA-DA-GCA}$ is the C/N ratio of the sugar unit after substitution with succinic anhydride. C/N_{GCA} is the C/N ratio of the deacetylated sugar unit.

2.5. Preparation of Amphiphilic Chitosan Nanomicelles

These were prepared using an ultrasonic self-assembly method [34]. One milligram of CS-DA-SA was dissolved in 10 mL of 1% acetic acid, followed by sonication for 10 min at room temperature, to prepare the CS-DA-SA-NMs.

2.6. Measurement of Particle Sizes and Zeta Potentials

Particle sizes, zeta potentials, and their distribution in the nanomicelles were evaluated using a Malvern nanoparticle size and potential analyzer (DLS). The CS-DA-SA-NMs were placed on the copper network and stained with a phosphotungstic acid negative staining solution for 2 min. The morphology of amphiphilic chitosan nanomicelles was examined under transmission electron microscopy (TEM).

2.7. Calculation of the Critical Micellar Concentration (CMC) of CS-DA-SA-NMs

The CMC values were evaluated using pyrene as a molecular probe [35]. A total of 4 mg of CS-DA-SA were dissolved in 10 mL of 1% acetic acid, followed by sonication for 10 min at room temperature, to yield 0.4 mg/mL of CS-DA-SA-NMs. This solution was diluted to varying concentrations of nanomicelles (0.2, 0.1, 0.05, 0.025, 0.0125, 0.00625, and 0.003125 mg/mL). Fifty microliters of 6×10^{-5} mg/mL pyrene/acetone solution were added to 5 mL of each of these dilutions. They were mixed and shaken well, followed by sonication for 15 min, heating (50 °C, 2 h), and incubation overnight at room temperature to reach equilibrium. The fluorescence spectra of different concentration polymer micelles were scanned using a fluorescence spectrophotometer with excitation at 339 nm. They were scanned between 360 and 450 nm using 5.0 nm slit widths for both excitation and emission.

2.8. Hemocompatibility of CS-DA-SA-NMs

The toxicity of nanomicelles was tested calorimetrically by hemoglobin release from erythrocytes, as described [36]. Specifically, blood was collected from SD rat hearts into heparinized tubes and centrifuged (3000 rpm, 10 min), followed by three saline washes and a resuspension of the erythrocytes to 2% (v/v) in saline. Two milliliters of the suspension were added to 2.0 mL of the CS-DA and CS-DA-SA solutions, followed by incubation (1 h, 37 °C) and centrifugation (3000 rpm, 15 min). The absorbances of the supernatants were determined at 540 nm using normal saline as the negative control (0% hemolysis) and ultrapure water as the positive control (100% hemolysis). The hemolysis percentage was determined using Equation (2).

$$\text{Hemolysis (\%)} = \frac{A_{\text{Sample}} - A_{\text{Saline}}}{A_{\text{Water}} - A_{\text{Saline}}} \times 100\% \quad (2)$$

2.9. Assays for Antimicrobial Activity Evaluation

2.9.1. Paper Diffusion

The described protocol [37] was used to assess the inhibition circles of CS, CS-DA, and CS-DA-SA. CS, CS-DA, and CS-DA-SA solutions of 0.125, 0.25, 0.5, 1, and 2 mg/mL were prepared using 0.2% acetic acid as solvent. *Escherichia coli* and *Staphylococcus aureus* were diluted to 10^6 CFU/mL using saline, and 1 mL of bacterial solution was added to the Petri dishes. Then, an LB agar medium was poured, and mixed well. After the addition of sterile 6 mm blank drug-sensitive tablets to the solid agar, the drug solution (20 μ L) was included with the drug-sensitive tablets. A total of 0.2% acetic acid and levofloxacin were the negative and positive controls, respectively, and the drug solution was diffused for 2 h in a refrigerator at 4 °C, followed by incubation for 24 h at 37 °C. The diameters of the inhibition zones (in mm) were determined by electronic vernier calipers. The experiment was repeated three times.

2.9.2. Measurement of Minimum Inhibitory Concentrations

These were measured for chitosan and chitosan derivatives against *E. coli* and *S. aureus* using the broth two-fold dilution method (the concentration corresponding to 90% inhibition). The rates of inhibition were calculated by counting the number of bacterial growth colonies in the nutrient agar dilution method. First, the prepared samples (dissolved in 0.2% acetic acid to make a mother liquor concentration of 2 mg/mL) were included with the bacterial culture solution (10^6 CFU/mL) so that the concentration of each test tube was 0, 0.0078125, 0.015625, 0.03125, 0.0625, or 0 mg/mL. Three parallel groups were set up by adding 4 μ L of *Escherichia coli* suspension or *Staphylococcus aureus* suspension to each of the seven concentration gradients in 96-well plates, followed by incubation for 12 h at 37 °C. A total of 100 μ L of bacterial cultures were removed and serially diluted with sterile saline to the predetermined concentrations. Finally, 1 mL of a bacterial solution was added to the culture dish, and then the LB agar medium was poured, mixed well, and incubated for 24 h at 37 °C. Live microbial colonies were obtained and counted.

2.9.3. Analysis of the Integrity of Bacterial Membranes

The integrity of the membranes was assessed by measuring DNA and RNA release from bacterial cells [38]. The method was modified according to a previous study [39]. The experiments were grouped into the control, CS (2 MIC), CS-DA (2 MIC), and CS-DA-SA (2 MIC) groups. The final concentration of the bacterial suspension was adjusted to 10^7 CFU/mL, and the test organisms were mixed with an equal volume of sample, followed by incubation for 12 h at 37 °C with shaking at 150 rpm/min. The suspensions were centrifuged (5000 rpm, 5 min, 4 °C), and absorbances at 260 nm were measured in the supernatants against an enzyme standard.

2.9.4. Effects of CS-DA-SA on Bacterial Morphology

The effects of CS, CS-DA, and CS-DA-SA on the morphology of *E. coli* and *S. aureus* were observed by SEM. As described [40] with some modifications, 3 mL of bacteria in stable or late-logarithmic growth were centrifuged (8000 rpm, 5 min), and the pelleted cells were fixed in 40 volumes of 2.5% glutaraldehyde at 4 °C for a minimum of 2 h. The bacteria were washed several times in a phosphate buffer and dehydrated (50, 70, and 90% ethanol). They were then resuspended in an ethanol tert-butanol solution (1:1, v/v) for 20 min. Finally, they were replaced twice with 100% tert-butanol, 20 min each time. After replacement, the samples were subjected to freeze-drying treatment, and the dried samples were observed and photographed using a scanning electron microscope (SEM) after being sprayed by an ion-sputtering apparatus.

2.9.5. Data Processing

OriginPro 2021 (OriginLab, Northampton, MA, USA) software was used for statistical analysis, and all data were expressed as $\bar{x} \pm s$. One-way ANOVA and LSD were used to

test the one-way variance; * $p < 0.05$ was considered a statistically significant difference and ** $p < 0.01$ was considered a highly significant difference.

3. Results and Discussion

3.1. Characterization of Chitosan Derivatives

The chitosan derivatives (CS-DA-SA) were successfully prepared (Figure S3). The structure of CS-DA-SA was evaluated and verified by FTIR, ^1H NMR, and XRD spectra (Figure S3A). The amphiphilic chitosan was successfully synthesized by introducing hydrophilic and hydrophobic groups into the $\text{C}_2\text{-NH}_2$ position of chitosan. The standard curve of the chitosan-free amino amount is shown in Figure 1, and the rate of deoxycholic acid grafting was calculated to be 23.93% by substituting it into the equation. The results of the elemental analysis of CS-DA and CS-DA-SA are presented in Table 1, and the grafting rate of succinic anhydride was measured as 29.25%.

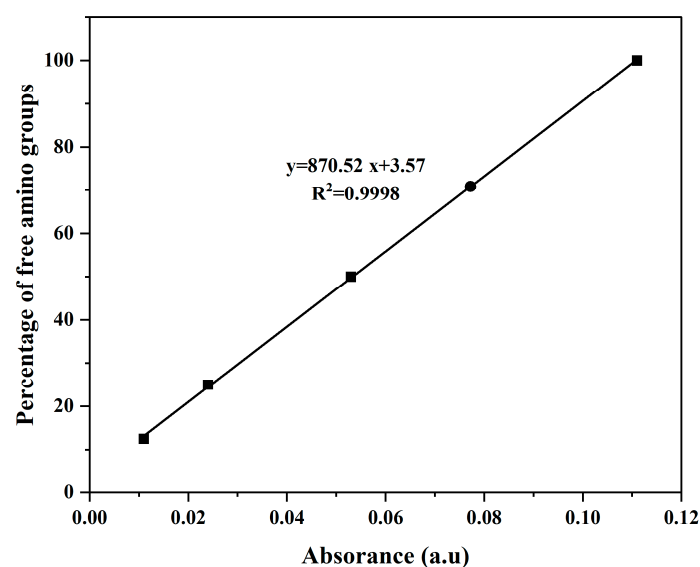


Figure 1. Standard curve of the free amino acid amount of chitosan.

Table 1. Elemental analysis table of CS-DA and CS-DA-SA.

Name	Element C (%)	Element H (%)	Element N (%)
CS-DA	42.64	6.99	7.4
CS-DA-SA	34.91	6.44	5.16

3.2. Measurement of the CMC

It is important that the concentration of the amphiphilic chitosan solution is higher or equal to the CMC to allow self-assembly of the polymers and their aggregation within shell-core structures. Pyrene is sensitive to microenvironmental polarities, and the ratio of the intensities of the first peak of its fluorescence spectrum (I_1 , 373 nm) to the third peak (I_3 , 383 nm) is used as a measure of these variations [41]. The CMC values of the amphiphilic chitosan nanomicelles are illustrated in Figure 2. The CMC of CS-DA-SA was found to be 0.05 mg/mL, indicating that CS-DA-SA can self-assemble to form nanomicelles at lower concentrations and more stable self-aggregation under dilution conditions [41]. The CMC values of CS-DA-SA were lower than similar amphiphilic chitosan nanocellulose systems, such as deoxycholic acid-O-carboxymethylated chitosan-folic acid affixes [42] and novel amphiphilic chitosan derivatives with hydrophilic carboxyl groups and hydrophobic hexadecyl groups [41].

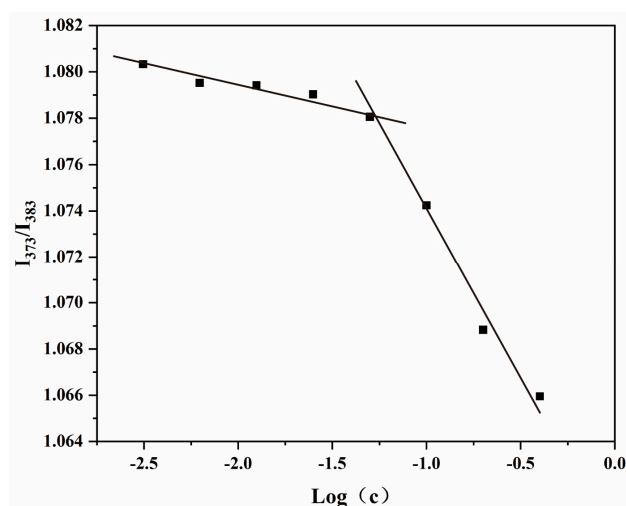


Figure 2. Critical micellar concentration of CS-DA-SA.

3.3. Particle Sizes, Zeta Potentials, and Morphological Analysis of Chitosan Derivatives

The addition of cationic or hydrophobic groups to chitosan usually leads to the acquisition of different physicochemical properties, including the capacity for nanoparticle self-assembly [25]. TEM was used for the morphological evaluation of the CS-DA-SA nanomicelles. As seen in Figure 3, the CS-DA-SA nanomicelles appeared spherical or quasi-spherical in shape with an even distribution. The self-assembly of CS-DA-SA resulted in nanoparticle diameters between 20 and 50 nm. However, shadowy structures were seen surrounding the particles in the TEM images. These may have been the result of flocculation during dehydration when the samples were prepared for TEM [43].

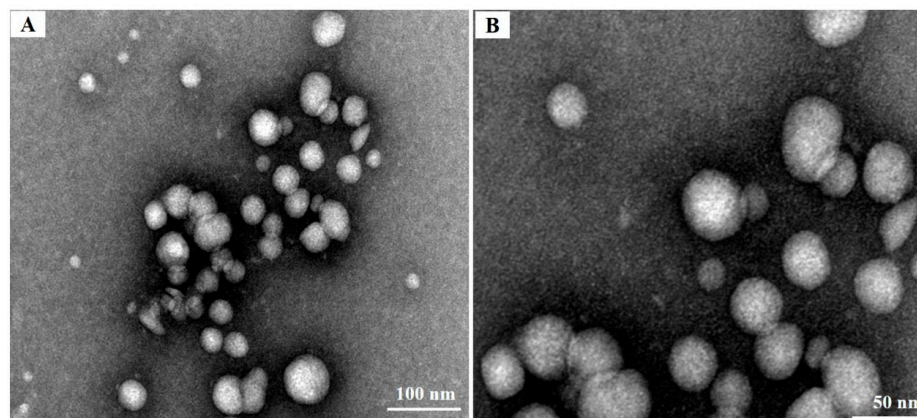


Figure 3. (A) TEM images of CS-DA-SA at a scale of 100 nm. (B): TEM images of CS-DA-SA at a scale of 50 nm.

Size and zeta potential are the basic characteristic parameters of nanosuspensions [44]. Table 2 shows the characteristics of CS-DA and CS-DA-SA-NMs. The diameter of CS-DA-SA-NMs nanomicelles was 827.47 ± 39.43 nm with a polydispersity index (PDI) of 0.93 ± 0.08 , indicating the narrow size distribution of the system. The zeta potential is a measure of surface charge and can significantly influence particle stability in solution due to inter-particle electrostatic repulsive forces [45]. The suspensions were considered stable when the zeta potentials were less than -15 mV or higher than $+15$ mV [46]. Both CS-DA and CS-DA-SA-NMs showed potentials greater than 15 mV, and CS-DA-SA-NMs were significantly higher. This indicates that CS-DA-SA-NMs are more stable and improve the stability of CS-DA.

Table 2. Zeta potentials and sizes of the synthesized CS-DA and CS-DA-SA.

Samples	Size (nm)	PDI	Zeta (mV)
CS-DA	1658.33 ± 192.02	0.74 ± 0.17	+25.97 ± 0.33
CS-DA-SA	827.47 ± 39.43	0.93 ± 0.08	+32 ± 0.28

PDI is the polydispersity index.

3.4. Hemocompatibility

Interactions between the free amino moieties of chitosan and cells or proteins in the circulation can lead to thrombosis or hemolytic reactions [47]. The contact of polymers with blood can be harmful or even instantly fatal [48], so it is important to determine the hemocompatibility of novel materials. Hemolysis is considered to be a very simple and reliable measurement to assess the hemocompatibility of materials. CS-DA and CS-DA-SA-NMs were incubated with erythrocytes separately to observe their effects on erythrocytes. The hemolysis rates were found to be $0.44 \pm 0.09\%$ for CS-DA and $0.16 \pm 0.13\%$ for CS-DA-SA-NMs, both of which are below the international standard of 5%, demonstrating good hemocompatibility in both. Wei-Yan Quan et al. [49] modified chitosan by an acylation reaction and grafted 18 β -glycyrrhetic acid and sialic acid, respectively, to synthesize amphiphilic chitosan, and found that the modified chitosan and the blood compatibility of sugar derivatives were significantly improved.

3.5. Antimicrobial Activity of CS-DA-SA

3.5.1. Agar Paper Sheet Diffusion

Previous studies have shown [22] that zeta potential has a strong influence on the antibacterial properties of nanoparticles, suggesting that these properties may result from interactions between the positively charged amino groups of chitosan with negative charges on the bacterial membrane. In this study, the inhibitory effects of CS, CS-DA, and CS-DA-SA on gram-negative (*E. coli*) and gram-positive (*S. aureus*) bacteria were investigated by paper diffusion method. The results of agar paper diffusion tests for the antibacterial activity of chitosan and its derivatives are presented in Table 3. It was found that varying concentrations of CS, CS-DA, and CS-DA-SA could inhibit the growth of both *E. coli* and *S. aureus*, with relatively similar inhibitory effects. Between 0.5 and 2 mg/mL, the inhibition effects of CS, CS-DA, and CS-DA-SA showed a concentration-dependent relationship. The inhibition effect of CS-DA-SA was significantly enhanced compared with CS and CS-DA. The possible reason is that the synthesized CS-DA-SA has an increased zeta potential value and an increased number of positive charges, thus enhancing its antibacterial ability. It is also possible that the antibacterial properties of CS were enhanced by the presence of succinic anhydride [22]. Jinping Cai et al. [50] synthesized a novel amphiphilic chitosan derivative, N-benzoyl-O-acetyl-chitosan (BACS). It was found that BACS also exhibited stronger antibacterial activity against *E. coli* and *S. aureus* compared to CS.

Table 3. Antibacterial activities of CS-DA against *E.coli* and *S.aureus*.

Strain	Concentration (mg/mL)	CS	CS-DA	CS-DA-SA	0.2% CH ₃ COOH	Levofloxacin
		Size of Inhibition Zone (mm)				
<i>S.aureus</i>	0.125	7.63 ± 0.21	7.47 ± 0.46	7.67 ± 0.31		
	0.25	8.53 ± 0.32	9.40 ± 0.26	7.43 ± 0.060		
	0.5	7.47 ± 0.21	8.33 ± 0.50	7.60 ± 0.26	0	9.90 ± 0.56
	1	7.67 ± 0.46	9.30 ± 0.36	9.47 ± 0.25		
	2	7.80 ± 0.20	8.80 ± 0.20	10.33 ± 0.32		
<i>E.coli</i>	0.125	7.03 ± 0.15	7.07 ± 0.23	8.03 ± 0.40		
	0.25	7.17 ± 0.15	7.40 ± 0.10	8.33 ± 0.06		
	0.5	7.13 ± 0.15	8.13 ± 0.38	8.03 ± 0.15	0	10.57 ± 0.38
	1	7.20 ± 0.20	8.43 ± 0.40	9.87 ± 0.42		
	2	7.33 ± 0.31	8.47 ± 0.25	10.80 ± 0.44		

3.5.2. Minimum Bacterial Inhibition Concentration

To determine the minimum concentration that can completely block bacterial growth, the minimum inhibitory concentrations of chitosan and its derivatives were determined after treatment of *E. coli* and *S. aureus* by the two-fold dilution method. The findings are illustrated in Table 4. Our results showed that the minimum inhibitory concentrations of CS-DA and CS-DA-SA-NMs were significantly lower and smaller compared to CS, indicating that CS-DA and CS-DA-SA improved the antibacterial activity of CS and had better antibacterial effects.

Table 4. MIC values of CS-DA and CS-DA-SA.

Strain	CS (mg/mL)	CS-DA (mg/mL)	CS-DA-SA (mg/mL)
<i>S.aureus</i>	0.125	0.0078125	0.015625
<i>E.coli</i>	0.125	0.0078125	0.015625

3.5.3. Microbial Growth Kinetics

To further verify the antimicrobial properties of chitosan and its derivatives, their effects on bacterial growth were evaluated using growth curves. The growth curves of the tested strains in the culture medium of chitosan and its derivatives are provided in Figure 4, indicating that the growth rates of both bacteria in the blank group showed an “S”-like curve. CS, CS-DA, and CS-DA-SA were effective in slowing bacterial growth in a short period (1–2 h), and the OD₆₀₀ values in the culture medium were small and changed very little after 2 h, indicating that they all had strong antibacterial effects. Overall, the OD₆₀₀ values of the bacterial cultures were ranked as CS > CS-DA > CS-DA-SA, indicating that the modified chitosan derivatives enhanced the antimicrobial properties of chitosan, which was consistent with the results of paper diffusion experiments.

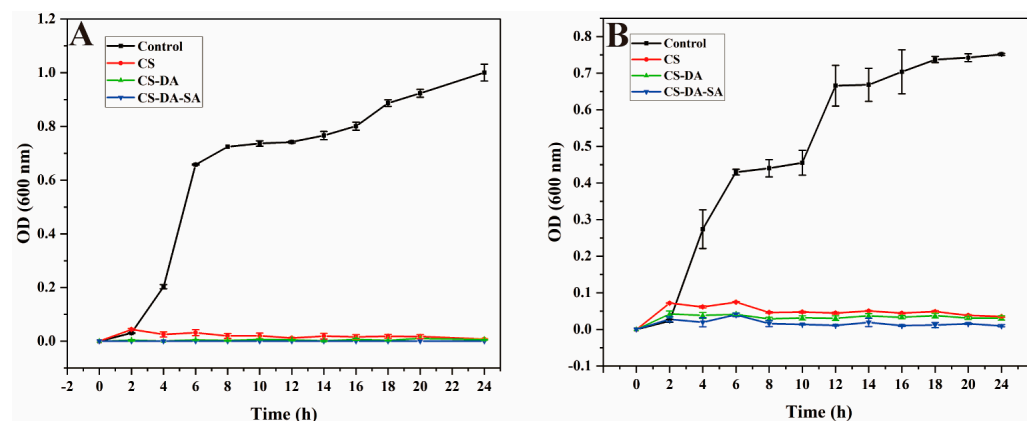


Figure 4. (A) Growth curves of *E. coli* after exposure to the control, CS, CS-DA, CS-DA-SA; (B): growth curves of *S. aureus* after exposure to the control, CS, CS-DA, CS-DA-SA.

3.5.4. Cell Membrane Integrity

The cell membrane is important for bacterial growth. Antibacterial agents can affect cell proliferation and differentiation, damage cell membranes, and leak small and macromolecular substances in cells [39,51]. The effects of chitosan and its derivatives on membrane integrity were revealed by measuring the amount of genetic material permeated from the cell membrane (Figure 5). It was found that compared with the blank group, both the CS and CS-DA-SA groups significantly increased the amount of DNA and RNA leakage of the intracellular genetic material of *Escherichia coli* and *Staphylococcus aureus* ($p < 0.01$). This indicated that CS and CS-DA-SA exerted an antibacterial effect by disrupting the integrity of the cell membrane. This is consistent with the results of Nuraziemah Ahmad et al. [25].

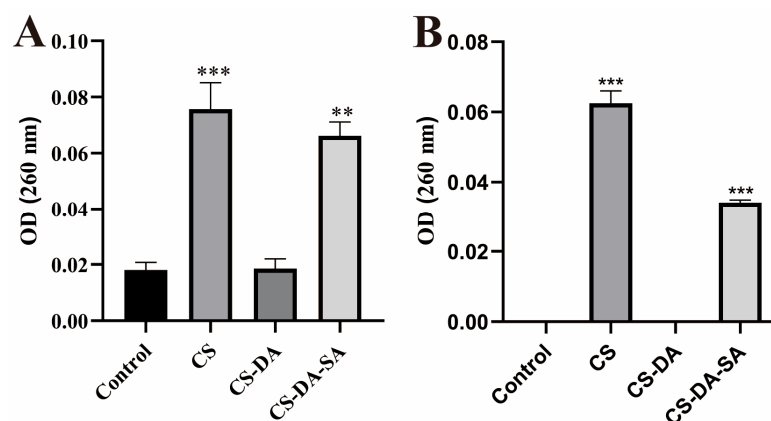


Figure 5. Absorption values at 260 nm for the release of nucleic acids (DNA and RNA) from *E. coli* (A) and *S. aureus* (B) treated in the control, CS, CS-DA, and CS-DA-SA groups. Versus the control group, ** $p < 0.01$, *** $p < 0.001$.

3.5.5. Scanning Electron Microscopy

Morphological changes in bacteria induced by chitosan and its derivatives were evaluated by SEM (Figure 6). The SEM maps of *E. coli* showed that the control bacteria were about 2 μm long, with bacillary form and smooth surface. The cell surface of the CS group was corrugated, and there were more pits inside the cells. The cell surface of the CS-DA and CS-DA-SA groups appeared depressed and distorted in shape. The cells of the CS-DA-SA group appeared crumpled, and some bacteria ruptured, probably because it could disrupt the bacterial cell membrane and prompt *E. coli* bacteria to crumple, lyse, and die. Shiqi He et al. [52] synthesized an amphiphilic polysiloxane ammonium salt (PDMS-g-AH), which also has a better inhibitory effect on *E. coli*, and the micelles formed by PDMS-g-AH have a high zeta potential, and the high positive charge density makes its binding ability to the bacterial cell membrane stronger so that it can easily interact with the microbial cell membrane. SEM images of *S. aureus* showed that the control group cells were about 0.8 μm in length, spherical in shape, smooth in surface, and arranged in grape bunches. The CS group cells were irregular in size, and more cells underwent rupture to produce fragments, probably due to disrupted cells or cell membrane dysfunction [53]. Most of the cells in the CS-DA group were divided and severely distorted, producing a large number of fragments. In the CS-DA-SA group of cells, some of the cells are divided to produce fragments. Another part of the cells was spherical and had a rough surface. The underlying antimicrobial mechanism may be the prevention of nutrient or oxygen entry into the bacterium due to membrane formation on the surface of the cell, thus inhibiting growth [54].

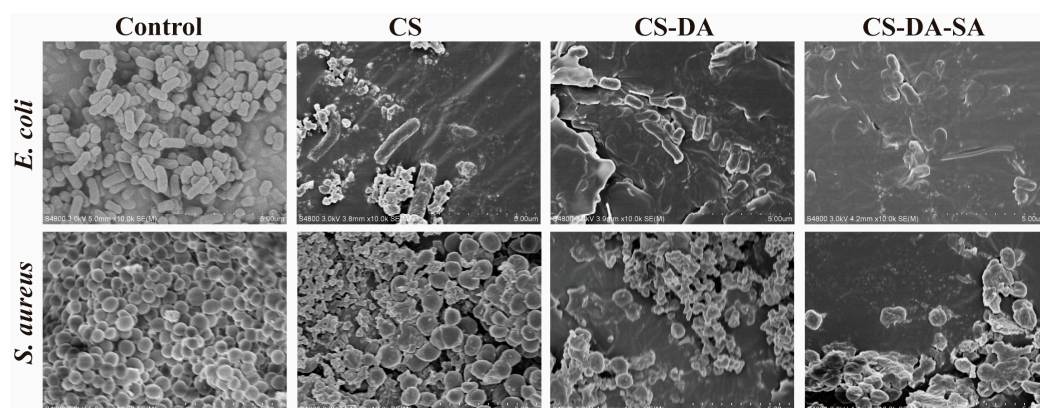


Figure 6. SEM morphology of *E. coli* and *S. aureus* in the control, CS, CS-DA, and CS-DA-SA groups at a scale of 5 μm .

4. Conclusions

This study synthesized novel amphiphilic chitosan by chemically modifying its structure with chitosan as a raw material, grafting the hydrophobic group DA and hydrophilic group SA at C₂-NH₂, respectively, and characterizing its structure. Ultrasonic self-assembly was used for the preparation of amphiphilic chitosan nanomicelles. The CMC of CS-DA-SA-NMs was found to be 0.05 mg/mL, indicating that they can form micelles at low concentrations. The particle size of CS-DA-SA-NMs was 827.47 ± 39.43 nm, the zeta potential was $+32 \pm 0.28$ mv, and the morphology was spherical. It was found that the modified chitosan derivatives, CS-DA and CS-DA-SA, both had strong antibacterial activity. The antibacterial activity of CS-DA and CS-DA-SA was significantly higher compared to CS, and the MIC values of CS-DA and CS-DA-SA were lower. CS-DA-SA may exert its antibacterial effect by disrupting the cell membrane or possibly forming a membrane on the cell surface. In conclusion, these results provide a theoretical foundation for the development of natural antimicrobial polymers into antimicrobial agents with improved and stable antimicrobial activity.

Supplementary Materials: The following supporting information can be downloaded at: <https://www.mdpi.com/article/10.3390/biom13111595/s1>. Figure S1: Synthesis route of CS-DA; Figure S2: Preparation of the chitosan functionalized with deoxycholic acid and succinic anhydride (CS-DA-SA); Figure S3: (A) FTIR spectra of CS, DA, SA, CS-DA, and CS-DA-SA; (B) ¹H NMR spectra of CS, DA, SA, CS-DA, and CS-DA-SA; (C) XRD spectra of CS, CS-DA, and CS-DA-SA. References [55–58] are cited in the supplementary materials.

Author Contributions: Software, Q.C.; Validation, L.L. and Z.H.; Formal analysis, Y.Q. and Y.J.; Resources, X.Z.; Data curation, X.C.; Writing—original draft, Q.O.; Project administration, K.W. and H.L.; Funding acquisition, H.L. All authors have read and agreed to the published version of the manuscript.

Funding: This work was supported by the Project of the Ph.D. Start-up Fund of Guangdong Medical University (GDMUB2021005), the Project of Traditional Chinese Medical of Guangdong Province (20232095), the science and technology innovation team project of Guangdong Provincial medical product Administration (2023TDZ12), the Key Discipline Construction Project of Guangdong Medical University (4SG23004G), Special Funds for the Economic Development of the Marine Economy of Guangdong Province, China (GDNRC (2022) 38), and the public service platform of the South China Sea for R&D marine biomedicine resources (2017C8A).

Institutional Review Board Statement: Not applicable.

Informed Consent Statement: Not applicable.

Data Availability Statement: The data are available from the corresponding author upon reasonable request.

Conflicts of Interest: The authors declare that they have no known competing financial interests or personal relationships that could have appeared to influence the work reported in this paper.

References

1. Fatima, F.; Siddiqui, S.; Khan, W.A. Nanoparticles as Novel Emerging Therapeutic Antibacterial Agents in the Antibiotics Resistant Era. *Biol. Trace Elem. Res.* **2021**, *199*, 2552–2564. [[CrossRef](#)]
2. Piegat, A.; Zywicka, A.; Niemczyk, A.; Goszczynska, A. Antibacterial Activity of N,O-Acylated Chitosan Derivative. *Polymers* **2020**, *13*, 107. [[CrossRef](#)]
3. Kamaruzzaman, N.F.; Tan, L.P.; Hamdan, R.H.; Choong, S.S.; Wong, W.K.; Gibson, A.J.; Chivu, A.; Pina, M.F. Antimicrobial Polymers: The Potential Replacement of Existing Antibiotics? *Int. J. Mol. Sci.* **2019**, *20*, 2747. [[CrossRef](#)]
4. Ramazanli, V.N. EFFECT OF pH AND TEMPERATURE ON THE SYNTHESIS OF SILVER NANO PARTICLES EXTRACTED FROM OLIVE LEAF. *Adv. Biol. Earth Sci.* **2021**, *6*, 169–173.
5. Nasibova, A. Generation of nanoparticles in biological systems and their application prospects. *Adv. Biol. Earth Sci.* **2023**, *8*, 140–146.
6. Ahire, S.A.; Bachhav, A.A.; Pawar, T.B.; Jagdale, B.S.; Patil, A.V.; Koli, P.B. The Augmentation of nanotechnology era: A concise review on fundamental concepts of nanotechnology and applications in material science and technology. *Results Chem.* **2022**, *4*, 100633. [[CrossRef](#)]

7. Zhang, Q.; Zhou, H.; Jiang, P.; Xiao, X. Metal-based nanomaterials as antimicrobial agents: A novel driveway to accelerate the aggravation of antibiotic resistance. *J. Hazard. Mater.* **2023**, *455*, 131658. [[CrossRef](#)]
8. Zhang, J.; Tang, W.; Zhang, X.; Song, Z.; Tong, T. An Overview of Stimuli-Responsive Intelligent Antibacterial Nanomaterials. *Pharmaceutics* **2023**, *15*, 2113. [[CrossRef](#)]
9. Jafarova, A.F.; Ramazanli, V.N. ANTIBACTERIAL CHARACTERISTICS OF Ag NANOPARTICLE EXTRACTED FROM OLIVE LEAF. *Adv. Biol. Earth Sci.* **2020**, *5*, 218–223.
10. Bakshi, P.S.; Selvakumar, D.; Kadirvelu, K.; Kumar, N.S. Chitosan as an environment friendly biomaterial—A review on recent modifications and applications. *Int. J. Biol. Macromol.* **2020**, *150*, 1072–1083. [[CrossRef](#)]
11. Baldelli, A.; Boraey, M.A.; Oguzlu, H.; Cidem, A.; Rodriguez, A.P.; Ong, H.X.; Jiang, F.; Bacca, M.; Thamboo, A.; Traini, D.; et al. Engineered nasal dry powder for the encapsulation of bioactive compounds. *Drug Discov. Today* **2022**, *27*, 2300–2308. [[CrossRef](#)] [[PubMed](#)]
12. Gao, F.; Hu, Y.; Gong, Z.; Liu, T.; Gong, T.; Liu, S.; Zhang, C.; Quan, L.; Kaveendran, B.; Pan, C. Fabrication of chitosan/heparinized graphene oxide multilayer coating to improve corrosion resistance and biocompatibility of magnesium alloys. *Mater. Sci. Eng. C* **2019**, *104*, 109947. [[CrossRef](#)] [[PubMed](#)]
13. Vasile, C.; Stoleru, E.; Darie-Nita, R.N.; Dumitriu, R.P.; Pamfil, D.; Tartau, L. Biocompatible Materials Based on Plasticized Poly(lactic acid), Chitosan and Rosemary Ethanol Extract I. Effect of Chitosan on the Properties of Plasticized Poly(lactic acid) Materials. *Polymers* **2019**, *11*, 941. [[CrossRef](#)]
14. Shih, P.Y.; Liao, Y.T.; Tseng, Y.K.; Deng, F.S.; Lin, C.H. A Potential Antifungal Effect of Chitosan against *Candida albicans* Is Mediated via the Inhibition of SAGA Complex Component Expression and the Subsequent Alteration of Cell Surface Integrity. *Front. Microbiol.* **2019**, *10*, 602. [[CrossRef](#)] [[PubMed](#)]
15. Avelelas, F.; Horta, A.; Pinto, L.F.V.; Cotrim Marques, S.; Marques Nunes, P.; Pedrosa, R.; Leandro, S.M. Antifungal and Antioxidant Properties of Chitosan Polymers Obtained from Nontraditional *Polybius henslowii* Sources. *Mar. Drugs* **2019**, *17*, 239. [[CrossRef](#)] [[PubMed](#)]
16. Azmana, M.; Mahmood, S.; Hilles, A.R.; Rahman, A.; Arifin, M.A.B.; Ahmed, S. A review on chitosan and chitosan-based bionanocomposites: Promising material for combatting global issues and its applications. *Int. J. Biol. Macromol.* **2021**, *185*, 832–848. [[CrossRef](#)]
17. Yan, D.; Li, Y.; Liu, Y.; Li, N.; Zhang, X.; Yan, C. Antimicrobial Properties of Chitosan and Chitosan Derivatives in the Treatment of Enteric Infections. *Molecules* **2021**, *26*, 7136. [[CrossRef](#)]
18. Hosseinnejad, M.; Jafari, S.M. Evaluation of different factors affecting antimicrobial properties of chitosan. *Int. J. Biol. Macromol.* **2016**, *85*, 467–475. [[CrossRef](#)]
19. Zhang, L.; Zhang, Z.; Li, C.; Hu, Z.; Liang, Y.; Yang, Z.; Cheng, Y.; Huang, D. Preparation and characterization of amphiphilic chitosan/iodine composite film as antimicrobial material. *Int. J. Biol. Macromol.* **2022**, *222*, 2426–2438. [[CrossRef](#)]
20. Verlee, A.; Mincke, S.; Stevens, C.V. Recent developments in antibacterial and antifungal chitosan and its derivatives. *Carbohydr. Polym.* **2017**, *164*, 268–283. [[CrossRef](#)]
21. Ye, Y.; Oguzlu, H.; Zhu, J.; Zhu, P.; Yang, P.; Zhu, Y.; Wan, Z.; Rojas, O.J.; Jiang, F. Ultrastretchable Ionogel with Extreme Environmental Resilience through Controlled Hydration Interactions. *Adv. Funct. Mater.* **2022**, *33*, 2209787. [[CrossRef](#)]
22. Li, Z.; Yang, F.; Yang, R. Synthesis and characterization of chitosan derivatives with dual-antibacterial functional groups. *Int. J. Biol. Macromol.* **2015**, *75*, 378–387. [[CrossRef](#)]
23. Li, J.; Zhuang, S. Antibacterial activity of chitosan and its derivatives and their interaction mechanism with bacteria: Current state and perspectives. *Eur. Polym. J.* **2020**, *138*, 109984. [[CrossRef](#)]
24. Tang, F.; Lv, L.; Lu, F.; Rong, B.; Li, Z.; Lu, B.; Yu, K.; Liu, J.; Dai, F.; Wu, D.; et al. Preparation and characterization of N-chitosan as a wound healing accelerator. *Int. J. Biol. Macromol.* **2016**, *93*, 1295–1303. [[CrossRef](#)]
25. Ahmad, N.; Wee, C.E.; Wai, L.K.; Zin, N.M.; Azmi, F. Biomimetic amphiphilic chitosan nanoparticles: Synthesis, characterization and antimicrobial activity. *Carbohydr. Polym.* **2021**, *254*, 117299. [[CrossRef](#)]
26. Huang, W.-T.; Chang, M.-C.; Chu, C.-Y.; Chang, C.-C.; Li, M.-C.; Liu, D.-M. Self-assembled amphiphilic chitosan: A time-dependent nanostructural evolution and associated drug encapsulation/elution mechanism. *Carbohydr. Polym.* **2019**, *215*, 246–252. [[CrossRef](#)]
27. Lu, Y.; Yue, Z.; Xie, J.; Wang, W.; Zhu, H.; Zhang, E.; Cao, Z. Micelles with ultralow critical micelle concentration as carriers for drug delivery. *Nat. Biomed. Eng.* **2018**, *2*, 318–325. [[CrossRef](#)]
28. Kong, W.; Jin, C.; Xiao, X.; Zhao, Y.; Li, Z.; Zhang, P.; Liu, W.; Li, X.F. Comparative study of effects of two bile acid derivatives on *Staphylococcus aureus* by multiple analytical methods. *J. Hazard. Mater.* **2010**, *179*, 742–747. [[CrossRef](#)]
29. Jiang, J.; Zhu, Y.; Zargar, S.; Wu, J.; Oguzlu, H.; Baldelli, A.; Yu, Z.; Saddler, J.; Sun, R.; Tu, Q.; et al. Rapid, high-yield production of lignin-containing cellulose nanocrystals using recyclable oxalic acid dihydrate. *Ind. Crops Prod.* **2021**, *173*, 114148. [[CrossRef](#)]
30. Oguzlu, H.; Danumah, C.; Boluk, Y. Colloidal behavior of aqueous cellulose nanocrystal suspensions. *Curr. Opin. Colloid Interface Sci.* **2017**, *29*, 46–56. [[CrossRef](#)]
31. Shi, Z.; Guo, R.; Li, W.; Zhang, Y.; Xue, W.; Tang, Y.; Zhang, Y. Nanoparticles of deoxycholic acid, polyethylene glycol and folic acid-modified chitosan for targeted delivery of doxorubicin. *J. Mater. Sci. Mater. Med.* **2014**, *25*, 723–731. [[CrossRef](#)]
32. Aiping, Z.; Tian, C.; Lanhua, Y.; Hao, W.; Ping, L. Synthesis and characterization of N-succinyl-chitosan and its self-assembly of nanospheres. *Carbohydr. Polym.* **2006**, *66*, 274–279. [[CrossRef](#)]

33. Wang, H.; Yang, Z.; He, Z.; Zhou, C.; Wang, C.; Chen, Y.; Liu, X.; Li, S.; Li, P. Self-assembled amphiphilic chitosan nanomicelles to enhance the solubility of quercetin for efficient delivery. *Colloids Surf. B Biointerfaces* **2019**, *179*, 519–526. [[CrossRef](#)]
34. Dong, E.; Yang, Z.; Zhou, C.; Wang, C.; Li, S.; Ouyang, Q.; Kong, L.; He, Z.; Xie, J.; Li, P.; et al. pH-responsive ultrasonic self-assembly spinosad-loaded nanomicelles and their antifungal activity to *Fusarium oxysporum*. *React. Funct. Polym.* **2019**, *141*, 123–132. [[CrossRef](#)]
35. Zhang, H.; Wang, K.; Zhang, P.; He, W.; Song, A.; Luan, Y. Redox-sensitive micelles assembled from amphiphilic mPEG-PCL-SS-DTX conjugates for the delivery of docetaxel. *Colloids Surf. B Biointerfaces* **2016**, *142*, 89–97. [[CrossRef](#)]
36. Li, X.; Yang, Z.; Yang, K.; Zhou, Y.; Chen, X.; Zhang, Y.; Wang, F.; Liu, Y.; Ren, L. Self-assembled polymeric micellar nanoparticles as nanocarriers for poorly soluble anticancer drug etaselen. *Nanoscale Res. Lett.* **2009**, *4*, 1502–1511. [[CrossRef](#)]
37. Shahbazi, Y. Chemical Composition and In Vitro Antibacterial Activity of *Mentha spicata* Essential Oil against Common Food-Borne Pathogenic Bacteria. *J. Pathog.* **2015**, *2015*, 916305. [[CrossRef](#)]
38. Chen, C.Z.; Cooper, S.L. Interactions between dendrimer biocides and bacterial membranes. *Biomaterials* **2002**, *23*, 3359–3368. [[CrossRef](#)]
39. Bouyahya, A.; Abrini, J.; Dakka, N.; Bakri, Y. Essential oils of *Origanum compactum* increase membrane permeability, disturb cell membrane integrity, and suppress quorum-sensing phenotype in bacteria. *J. Pharm. Anal.* **2019**, *9*, 301–311. [[CrossRef](#)]
40. Li, Q.; Zhang, W.; Liao, S.; Xing, D.; Xiao, Y.; Zhou, D.; Yang, Q. Mechanism of lead adsorption by a *Bacillus cereus* strain with indole-3-acetic acid secretion and inorganic phosphorus dissolution functions. *BMC Microbiol.* **2023**, *23*, 57. [[CrossRef](#)]
41. Li, W.; Peng, H.; Ning, F.; Yao, L.; Luo, M.; Zhao, Q.; Zhu, X.; Xiong, H. Amphiphilic chitosan derivative-based core-shell micelles: Synthesis, characterisation and properties for sustained release of Vitamin D3. *Food Chem.* **2014**, *152*, 307–315. [[CrossRef](#)] [[PubMed](#)]
42. Wang, F.; Zhang, D.; Duan, C.; Jia, L.; Feng, F.; Liu, Y.; Wang, Y.; Hao, L.; Zhang, Q. Preparation and characterizations of a novel deoxycholic acid-O-carboxymethylated chitosan-folic acid conjugates and self-aggregates. *Carbohydr. Polym.* **2011**, *84*, 1192–1200. [[CrossRef](#)]
43. Ahn, S.; Lee, S.J. Dehydration-mediated cluster formation of nanoparticles. *Sci. Rep.* **2015**, *5*, 11383. [[CrossRef](#)] [[PubMed](#)]
44. Du, W.-L.; Niu, S.-S.; Xu, Y.-L.; Xu, Z.-R.; Fan, C.-L. Antibacterial activity of chitosan tripolyphosphate nanoparticles loaded with various metal ions. *Carbohydr. Polym.* **2009**, *75*, 385–389. [[CrossRef](#)]
45. Qi, L.; Xu, Z.; Jiang, X.; Hu, C.; Zou, X. Preparation and antibacterial activity of chitosan nanoparticles. *Carbohydr. Res.* **2004**, *339*, 2693–2700. [[CrossRef](#)] [[PubMed](#)]
46. Parveen, S.; Rana, S.; Fangueiro, R.; Paiva, M.C. Characterizing dispersion and long term stability of concentrated carbon nanotube aqueous suspensions for fabricating ductile cementitious composites. *Powder Technol.* **2017**, *307*, 1–9. [[CrossRef](#)]
47. Balan, V.; Verestiuc, L. Strategies to improve chitosan hemocompatibility: A review. *Eur. Polym. J.* **2014**, *53*, 171–188. [[CrossRef](#)]
48. Liu, Z.; Jiao, Y.; Wang, T.; Zhang, Y.; Xue, W. Interactions between solubilized polymer molecules and blood components. *J. Control. Release* **2012**, *160*, 14–24. [[CrossRef](#)]
49. Quan, W.Y.; Kong, S.Z.; Li, S.D.; Liu, H.Z.; Ouyang, Q.Q.; Huang, Y.M.; Luo, H. Grafting of 18beta-Glycyrrhetic Acid and Sialic Acid onto Chitosan to Produce a New Amphipathic Chitosan Derivative: Synthesis, Characterization, and Cytotoxicity. *Molecules* **2021**, *26*, 452. [[CrossRef](#)]
50. Cai, J.; Dang, Q.; Liu, C.; Fan, B.; Yan, J.; Xu, Y.; Li, J. Preparation and characterization of N-benzoyl-O-acetyl-chitosan. *Int. J. Biol. Macromol.* **2015**, *77*, 52–58. [[CrossRef](#)]
51. Xie, Y.; Zhang, C.; Mei, J.; Xie, J. Antimicrobial Effect of *Ocimum gratissimum* L. Essential Oil on *Shewanella putrefaciens*: Insights Based on the Cell Membrane and External Structure. *Int. J. Mol. Sci.* **2023**, *24*, 11066. [[CrossRef](#)] [[PubMed](#)]
52. He, S.; Hou, M.; Shan, S.; Li, R.; Yu, N.; Lin, Y.; Zhang, A. Synthesis and anti-bacterial/fungal activities of amphiphilic polysiloxanes primary ammonium salts. *React. Funct. Polym.* **2023**, *183*, 105495. [[CrossRef](#)]
53. Guimaraes, A.C.; Meireles, L.M.; Lemos, M.F.; Guimaraes, M.C.C.; Endringer, D.C.; Fronza, M.; Scherer, R. Antibacterial Activity of Terpenes and Terpenoids Present in Essential Oils. *Molecules* **2019**, *24*, 247. [[CrossRef](#)] [[PubMed](#)]
54. Maliszewska, I.; Czapka, T. Electrospun Polymer Nanofibers with Antimicrobial Activity. *Polymers* **2022**, *14*, 1661. [[CrossRef](#)] [[PubMed](#)]
55. Wu, M.; Guo, K.; Dong, H.; Zeng, R.; Tu, M.; Zhao, J. In vitro drug release and biological evaluation of biomimetic polymeric micelles self-assembled from amphiphilic deoxycholic acid-phosphorylcholine-chitosan conjugate. *Mater. Sci. Eng. C-Mater. Biol. Appl.* **2014**, *45*, 162–169. [[CrossRef](#)] [[PubMed](#)]
56. Niu, X.; Zhu, L.; Xi, L.; Guo, L.; Wang, H. An antimicrobial agent prepared by N-succinyl chitosan immobilized lysozyme and its application in strawberry preservation. *Food Control* **2020**, *108*, 106829. [[CrossRef](#)]
57. Zidan, T.A.; Abdelhamid, A.E.; Zaki, E.G. N-Aminorhodanine modified chitosan hydrogel for antibacterial and copper ions removal from aqueous solutions. *Int. J. Biol. Macromol.* **2020**, *158*, 32–42. [[CrossRef](#)] [[PubMed](#)]
58. Han, X.; Zheng, Z.; Yu, C.; Deng, Y.; Ye, Q.; Niu, F.; Chen, Q.; Pan, W.; Wang, Y. Preparation, characterization and antibacterial activity of new ionized chitosan. *Carbohydr. Polym.* **2022**, *290*, 119490. [[CrossRef](#)]

Disclaimer/Publisher's Note: The statements, opinions and data contained in all publications are solely those of the individual author(s) and contributor(s) and not of MDPI and/or the editor(s). MDPI and/or the editor(s) disclaim responsibility for any injury to people or property resulting from any ideas, methods, instructions or products referred to in the content.